MODELS AND PARAMETERS FOR THE COUPLED DIFFUSION OF DOPANTS AND POINT DEFECTS IN SILICON

Scott T. Dunham and Frederick P. Wittel
Boston University
Electrical, Computer, and Systems Engineering Dept.
Boston, MA 02215

Abstract

Coupled diffusion models for dopants and point defects provide an essential foundation for simulation of more complicated processes. In this work, we develop consistent quantitative models for coupled diffusion by combining physical models for bulk and interface interactions of dopants and defects with parameter characterization based on a wide range of experimental results.

INTRODUCTION

Understanding and modeling the coupled diffusion of dopants and point defects is critical for the continuing evolution of VLSI technology, as these processes provide the foundation for more complicated processes, such as ion implant annealing or dopant precipitation. However, the development of consistent quantitative models remains a challenge due to the complexity of the interactions involved, the large number of parameters, and the difficulty in making direct measurements of critical properties. In this work, we show that by developing physical models of dopant/defect interactions and quantifying those models using a wide range of experiments designed to extract specific model parameters, it is possible to build up a consistent system which can effectively model the wide array of experimental behavior.

PAIR DIFFUSION MODEL

The current standard model for coupled dopant/defect diffusion is the pair diffusion model [1, 2], which assumes that dopant diffusion occurs through the formation of dopant/defect pairs which then diffuse as a unit. Assuming dopant/defect pairing and ionization reactions to be near local equilibrium, the system can be written as:

$$\frac{\partial^2 \left(C_{\mathrm{A}} + C_{(\mathrm{AI})} + C_{(\mathrm{AV})}\right)}{\partial t} = -\nabla \cdot \left(J_{(\mathrm{AI})} + J_{(\mathrm{AV})}\right) \tag{1}$$

$$\frac{\partial^2 \left(C_{\mathrm{I}} + C_{(\mathrm{AI})}\right)}{\partial t} = -\nabla \cdot \left(J_{\mathrm{I}} + J_{(\mathrm{AI})}\right) - R \tag{2}$$

$$\frac{\partial^2 \left(C_{\mathrm{V}} + C_{(\mathrm{AV})}\right)}{\partial t} = -\nabla \cdot \left(J_{\mathrm{V}} + J_{(\mathrm{AV})}\right) - R, \tag{3}$$

where C_{I}, C_{V}, $C_{(\mathrm{AI})}$ and $C_{(\mathrm{AV})}$ represent the concentrations of point defects and pairs summed over all their charge states and the net recombination rate can be written

$$R = k_{\mathrm{I/V}} \left(C_{\mathrm{I}} C_{\mathrm{V}} - C_{\mathrm{I}}^* C_{\mathrm{V}}^*\right). \tag{4}$$

The flux terms include sums over all the charge states, so for example:

$$J_{(\mathrm{AV})} = -\left[\sum_i D_{\mathrm{A}}^{\mathrm{V}^i} \left(\frac{n_i}{n}\right)^i\right] \left[\nabla C_{\mathrm{A}} + \frac{C_{\mathrm{A}}}{C_{\mathrm{V}^0}} \nabla C_{\mathrm{V}^0}\right] \tag{5}$$

where $D_{\mathrm{A}}^{\mathrm{V}^i}$ is the diffusivity of a dopant via vacancies of charge i.

Although this model is appropriate for diffusion via interstitial mechanisms, lattice Monte-Carlo (LMC) simulations show that because a dopant/vacancy pair must partially dissociate to diffuse, at least two deviations from basic pair diffusion should be considered for vacancy-mediated diffusion [3, 4]. First, interactions of vacancies with multiple dopants leads to a rapid increase in dopant diffusivity at very high donor levels so that the $D_{\mathrm{A}}^{\mathrm{V}^i}$ in Eq. (5) should be multiplied by a factor

$$[1 + (C_D/C^*)^m] \tag{6}$$

with $m \sim 3$. This change leads to a rapid rise in diffusivity for donor concentrations above about $2 \times 10^{20}\mathrm{cm}^{-3}$ as observed experimentally [5]. Figure 1 shows a match of this model to experimental data, with the values for the parameters C^* and m taken from the results of LMC simulations [3]. Second, since pairs are not perfectly bound, the effect of a vacancy gradient on dopant diffusion is weaker than predicted by Eq. (5) such that the last term should be multipled by a factor $1 > \gamma > -2$, depending on the strength of the dopant/vacancy interaction (1 for very strong interaction, -2 for no interaction) [4].

These equations provide the basis for the point defect-based models in process simulators such as SUPREM IV [6]. However, a major challenge is determining the large set of required model parameters as well as boundary conditions such that these equations are consistent with the range of experimental observations made on the silicon system. The next few sections will discuss how such parameters can be extracted from experiments designed to be selectively sensitive to small subsets of the parameter set.

POINT DEFECT PROPERTIES

In quantifying parameters, it is appropriate to start with point defect properties. Although reported values for point defect parameters as extracted from experiments vary widely, if the effective interface recombination velocity is assumed to decrease with time, it is possible to account for the low effective interstitial diffusivities extracted from lateral OED [8] or backside OED experiments [9] using a high interstitial diffusivity (such as that determined from metal diffusion experiments [10, 11, 12]). Further support for the effective interface regrowth velocity being time-dependent comes from reverse short channel effect results of Rafferty *et al.* [13, 14] and measurements of non-uniform OED in SOI structures by Crowder *et al.* [15]. In both cases, to match the results of these low thermal budget processes, it is necessary to use a much larger regrowth velocity than is consistent with longer time experiments [8, 9].

Rogers and Massoud [16] were able to match stacking fault growth during backside oxidation by assuming a time-dependent interface regrowth velocity for interstitials of the form $\sigma_{\rm I} = A\,t^{-n}$ ($n \sim 1$), but propose no physical explanation for the behavior. If interstitials are assumed to preferentially segregate to surface oxide films, as implied by OED models [17, 18, 19], then considering this segregation (along with slow diffusion in the oxide) during annealing processes leads to an effective interface regrowth velocity that decreases with time since the flux of interstitials into the oxide slows as the near-interface region fills with excess silicon. By including segregation of point defects from silicon to SiO_2 and parameters for silicon diffusion in SiO_2 from thermomigration data [20, 21, 22], it is possible to quantitatively match the full range of experimental results (lateral OED, backside OED, buried layer OED, etc.) [23] using point defect properties from metal diffusion [10]. Figure 2 shows an example of using this model to match lateral OED experiments of Griffin [8].

As the doping level changes, the equilibrium concentrations of charged point defects change. These changes in equilibrium point defect concentrations as the Fermi level is changed are still not well-established. We use the values for the point defect ionization levels that are most commonly cited. The vacancy levels are taken from the low-temperature EPR results of Watkins [24], while interstitial levels extracted from OED in doped silicon [25] are used. Calculating the vacancy ionization energies at diffusion temperatures requires assumptions for how the states shift within the gap as temperature changes (and the gap shrinks), while calculations of the interstitial defect levels depend of assumptions about how interstitial injection during oxidation is affected by substrate doping. For vacancies, the resulting values for the negative ionization levels are closer than the positive levels to the intrinsic Fermi level, so the equilibrium vacancy concentration increases most rapidly in n-type material, while for interstitials, the equilibrium concentration increases most rapidly for p-type material, since the positive ionization level is closer to mid-gap.

Recent OED/ORD observations [30, 31] provide a lower limit for the rate of bulk recombination, which imply that the reaction barrier is small. It should be noted that the effective value of $k_{I/V}$ can be expected to depend on doping, with the reaction of dopant/defect pairs with opposite type defects and the expected repulsion of like-charged defects causing increases and decreases, respectively, as doping increases. Given these compensating effects and the lack of experiments to provide further characterization, we assume a constant value for $k_{I/V}$, independent of doping.

DOPING LEVEL DEPENDENCE

As indicated by the sum over defect charge states in Eq. (5), dopant diffusivity (for donors) is commonly written as

$$D_{\mathrm{A}} = D_{\mathrm{A}}^{0} + D_{\mathrm{A}}^{-}\left(\frac{n}{n_i}\right) + D_{\mathrm{A}}^{=}\left(\frac{n}{n_i}\right)^2, \tag{7}$$

where the three terms represent diffusion via neutral, negative and double-negative defects (signs are reversed for acceptors). Figures 3 and 4 show measured diffusivities as a function of Fermi level from recent isoconcentration diffusion data for phosphorus and boron in boron, phosphorus and arsenic backgrounds [26, 27]. A couple of observations are readily apparent. First, although widely-used parameters (e.g., in SUPREM IV) for phosphorus diffusivity include a strong $(n/ni)^2$ dependence [28], there is no indication of such behavior in these experiments. The model fits include only the first two terms in Eq. (7). It should be noted that the highest doping levels attained in these experiments are insufficient to expect significant contribution from very high concentration effects as in Eq. (6). Second, in oppositely-doped material, both phosphorus and boron show substantially reduced diffusion, much less than is consistent with Fermi level effects alone. This behavior can be accounted for by including donor/acceptor pairing, which immobilizes a fraction of the dopants, thereby reducing the effective diffusivities beyond that expected from Fermi level effects alone [26, 27]. To include donor/acceptor pairing in the model described above, the concentration of pairs (C_{AB}) can be added to the total dopant concentration in the time derivative on the left-hand-side of Eq. (1), with $C_{\mathrm{AB}} = K_{\mathrm{AB}} C_{\mathrm{A}} C_{\mathrm{B}}$.

Observations of enhanced/retarded diffusion of different dopants during oxidation/nitridation [29] allows determination of the relative importance of interstitial versus vacancy diffusion mechanisms under intrinsic conditions ($f_{\mathrm{I}} = D_{\mathrm{A}}^{\mathrm{I}}/(D_{\mathrm{A}}^{\mathrm{I}} + D_{\mathrm{A}}^{\mathrm{V}})$). This information is complementary to isoconcentration experiments (Figs. 3 and 4) which do not distinguish between interstitial and vacancy mechanisms, but allow determination of the relative importance of different charge states for diffusion. Combined with estimates of how f_{I} changes with Fermi level, these experiments provide the information required to characterize the parameters in the dopant flux equations (e.g., Eq. (5)).

HIGH CONCENTRATION DIFFUSION

The system as quantified based on these experiments designed to isolate parameters can be applied to the evolution of high concentration diffusion profiles. The remaining parameter which remains unquantified is I/V recombination, which we retain as the lone fitting parameter. The resulting model is effective in accounting for the differences in diffusion behavior between the different dopants.

As shown for example in Figs. 5 and 6, the model matches phosphorus profiles spanning a broad range of doping levels (intrinsic to solubility) and temperatures, including "kink and tail" features [27]. The plateau observed for very high doping levels arises in the model from the strong dependence of vacancy-mediated diffusivity on doping as predicted from LMC simulations. The extracted bulk recombination is slightly smaller than diffusion-limited. When the same models and point defect parameters are applied to other dopants, they accurately predict differences in diffusion behavior. Because of lower diffusivities, arsenic and antimony show standard concentration-dependent behavior, while boron shows substantial enhanced tail diffusion, all matching experimental observations. Thus, the model and parameter characterization described in this work provides a consistent quantitative approach to coupled dopant/defect diffusion.

CONCLUSIONS

In summary, although significant gaps in our knowledge still remain, by characterizing coupled dopant/defect diffusion models based on experiments designed to isolate specific parameter values, it is possible to build up a consistent system for dopant/defect diffusion which accounts for a wide range of observed behavior.

ACKNOWLEDGMENT

This work was supported by SRC grants SJ-530 and BJ-530.

REFERENCES

[1] D. Mathiot and J. C. Pfister, *J. Appl. Phys.* **55**, 3518 (1984).

[2] M. Yoshida, *Jap. J. Appl. Phys.* **22**, 1404 (1983).

[3] S.T. Dunham and C.D. Wu, *J. Appl. Phys.* **78**, 2362 (1995).

[4] S.T. Dunham and C.D. Wu, in **SISDEP'95 Proc.**.

[5] A. Nylandsted Larsen, K. Kyllesbech Larsen, P. E. Andersen, B. G. Svensson, *J. Appl. Phys.* **73**, 691 (1993).

[6] M. E. Law and R. W. Dutton, *IEEE Trans. Comp. Aid. Des.*, 181 (1987).

[7] R. B. Fair in **Impurity Doping Processes in Silicon**, ed. F. F. Y. Yang (North-Holland, New York, 1981) p. 315.

[8] P. B. Griffin and J. D. Plummer, *Proceedings of the Electrochemical Society Meeting*, San Diego, CA, October 1986.

[9] S. T. Ahn, J. D. Shott and W. A. Tiller, *Proceedings of the Electrochemical Society Meeting*, San Diego, CA, October 1986.

[10] H. Bracht, N. A. Stolwijk and H. Mehrer, in **Semiconductor Silicon/1994** (Electrochem. Soc. Proc. Vol. **94-10**) pp. 593-602B.

[11] F. Morehead, in **Defects in Electronic Materials**, M. Stavola, S. J. Pearton and G. Davies, eds. (Mat. Soc. Proc. **104**, Pittsburgh, PA, 1988) p. 99-104.

[12] H. Zimmermann and H. Ryssel, *Appl. Phys. A* **55**, 121 (1992).

[13] C. S. Rafferty, M. D. Giles, H.-H. Vuong, S. A. Eshraghi, M. R. Pinto and S. J. Hillenius, in **1993 International Workshop on VLSI Process and Device Modeling (VPAD 1993)**, K. Asada, ed. (Japan, 1993) pp. 148-149.

[14] C. S. Rafferty, S. A. Eshraghi, M. R. Pinto, S. J. Hillenius and H.-H. Vuong, #12.6 IEDM 1993 Proceedings.

[15] S. Crowder, P. B. Griffin and J. D. Plummer, in **Process Physics and Modeling in Semiconductor Technology**, G. R. Srinivasan, K. Taniguchi and C. S. Murthy, eds. (Electrochem. Soc. Proc. Vol. **93-6**, Pennington, NJ, 1993) pp. 108-119.

[16] W. B. Rogers and H. Z. Massoud, *J. Electrochem. Soc.* **138**, 3483 (1991).

[17] S. T. Dunham and J. D. Plummer, *J. Appl. Phys.* **57**, 2541 (1986).

[18] S. T. Dunham, *J. Electrochem. Soc.* **136**, 250 (1989).

[19] S. T. Dunham, *J. Appl. Phys.* **71**, 685 (1991).

[20] G. K. Celler, L. E. Trimble, T. T. Sheng, S. G. Kosinski and K. W. West, *Appl. Phys. Lett.* **53**, 1178 (1988).

[21] G. K. Celler and L. E. Trimble, *Appl. Phys. Lett.* **53**, 2492 (1988).

[22] G. K. Celler and L. E. Trimble, *Appl. Phys. Lett.* **54**, 1427 (1989).

[23] A.M. Agarwal and S.T. Dunham, *J. Appl. Phys.* **78**, 5313 (1995)

[24] G. D. Watkins, in **Lattice Defects in Semiconductors 1974**, Inst. Phys. Conf. Ser. 23, London, 1975.

[25] M. D. Giles, *IEEE Trans. CAD* **8**, 460 (1989).

[26] F.P. Wittel and S. T. Dunham, *Appl. Phys. Lett.* **66**, 1415 (1995).

[27] F.P. Wittel, Ph.D. Thesis, Boston Univ. (1995).

[28] R. Fair and W. Meyer, in **Silicon processing ASTM STP 804**, 1983.

[29] P. Fahey, G. Barbuscia, M. Moslehi and R. W. Dutton, *Appl. Phys. Lett.* **43**, 683 (1983).

[30] E. Guerrero, W. Jüngling, H. Pötzl, U. Gösele, M. Grasserbauer and G. Stingeder, *J. Electrochem. Soc.* **133**, 2181 (1986).

[31] P. A. Packan, PhD thesis, Stanford University, February 1991.

[32] M. Yoshida, *Jap. J. Appl. Phys.* **18**, 479 (1979).

[33] S. Matsumoto, M. Yoshida asnd T. Niimi, *Jap. J. Appl. Phys.* **13**, 1899 (1974).

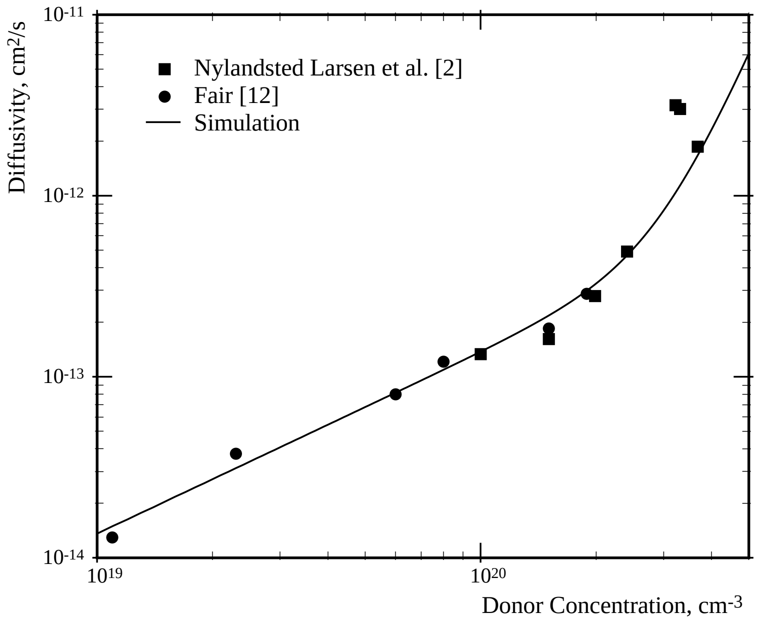

Figure 1: Comparison of experimental measurement [5, 7] of arsenic diffusivity at 1050°C versus doping level to lattice Monte-Carlo simulations. The diffusivity for moderate doping levels is fit assuming diffusion via negatively-charged vacancies and then extrapolated to higher doping levels using the simulation results.

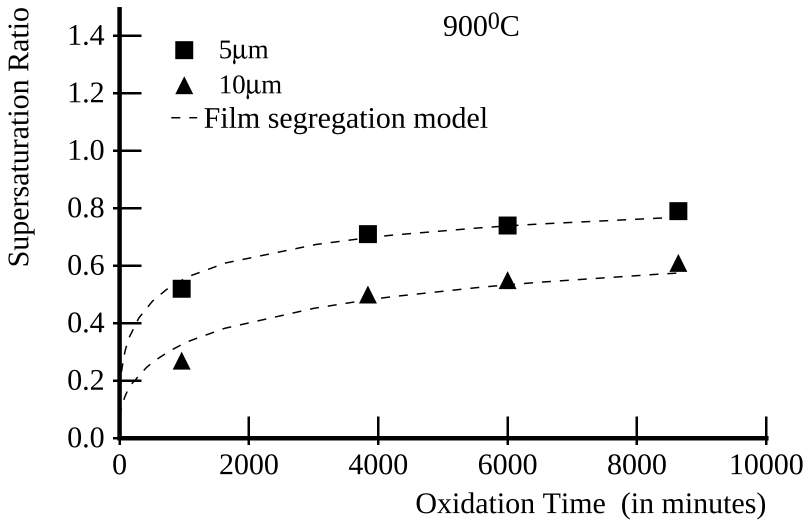

Figure 2: Comparison of model to relative diffusivity enhancement versus time for boron near the center of nitride/oxide stripes serving as oxidation barriers during local oxidation at 900°C. Data from Griffin *et al.* [8].

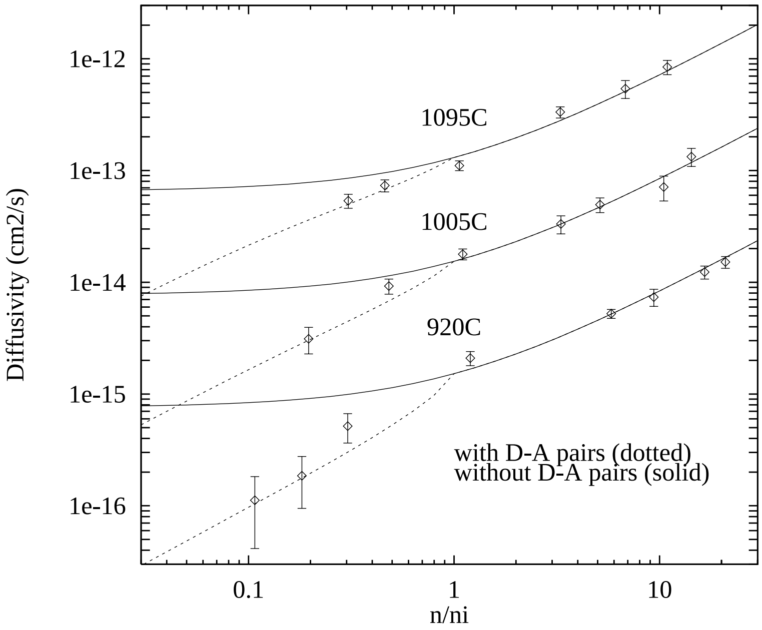

Figure 3: Diffusivity versus Fermi level of phosphorus marker layer in arsenic and boron backgrounds. Comparison to model with and without donor/acceptor pairing.

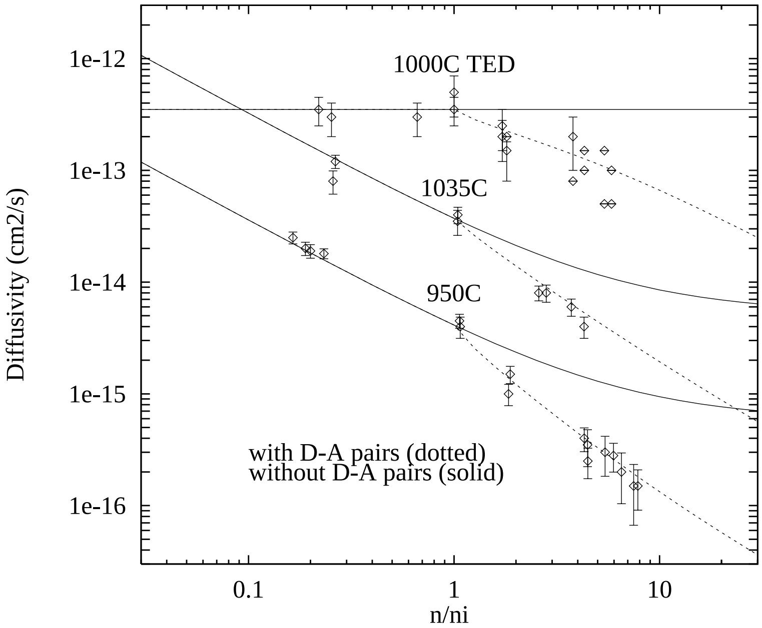

Figure 4: Diffusivity versus Fermi level of boron marker layer in arsenic, phosphorus and boron backgrounds. Comparison to model with and without donor/acceptor pairing. Also included is average diffusivity during 20s 1000°C RTA anneal following implant.

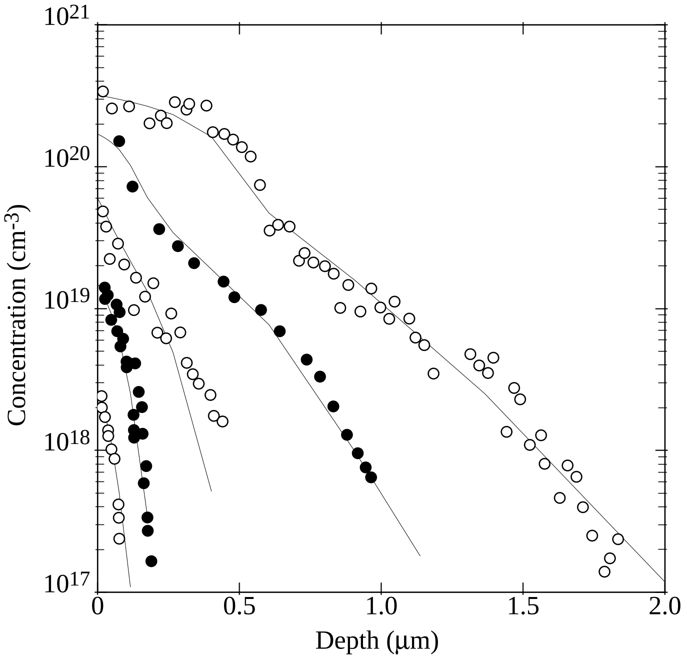

Figure 5: Phosphorus diffusion profiles for 4 h at 900°C from Yoshida [32] and Matsumoto *et al.* [33] and comparison to simulation results.

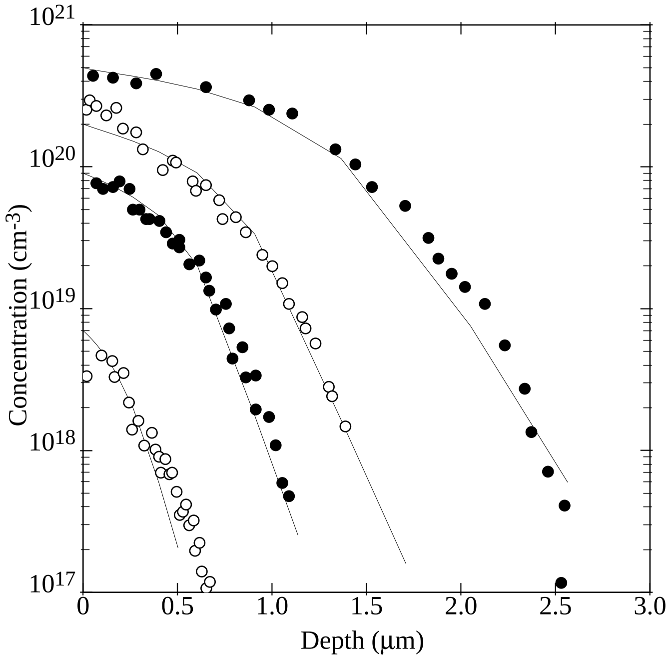

Figure 6: Phosphorus diffusion profiles for 30 min at 1100°C from Yoshida [32] and Matsumoto *et al.* [33] and comparison to simulation results.

KEYWORDS

Dopant diffusion, point defects, isoconcentration, dopant/dopant pairing, coupled diffusion